# A shared role for sonic hedgehog signalling in patterning chondrichthyan gill arch appendages and tetrapod limbs

**Running title:** Shh signalling patterns skate gill arches

J. Andrew Gillis[1,2*] and Brian K. Hall[3]

1. Department of Zoology, University of Cambridge, Downing Street, Cambridge, CB2 3EJ, U.K.
2. Marine Biological Laboratory, 7 MBL Street, Woods Hole, MA, U.S.A.
3. Department of Biology, Dalhousie University, 1355 Oxford Street, Halifax, Nova Scotia, B3H 4R2, Canada

* Correspondence: jag93@cam.ac.uk

**Key words:** Sonic hedgehog, gill arch, evolution, skate, appendage patterning

**Summary statement:** Shh signalling polarizes skate gill arches, and maintains proliferative expansion of gill arch appendage endoskeletal progenitors, mirroring the function of Shh signalling in the tetrapod limb.

**Chondrichthyans (sharks, skates, rays and holocephalans) possess paired appendages that project laterally from their gill arches, known as "branchial rays". This led Carl Gegenbaur to propose that paired fins (and hence tetrapod limbs) originally evolved via transformation of gill arches. Tetrapod limbs are patterned by a *Sonic hedgehog (Shh)*-expressing signalling centre known as the zone of polarizing activity, which establishes the anteroposterior axis of the limb bud, and maintains proliferative expansion of limb endoskeletal progenitors. Here, we use loss of function, label-retention and fate-mapping approaches in the little skate to demonstrate that Shh secretion from a signalling centre in the developing gill arches establishes gill arch anteroposterior polarity and maintains the proliferative expansion of branchial ray endoskeletal progenitor cells. These findings highlight striking parallels in the axial patterning mechanisms employed by chondrichthyan branchial rays and paired fins/limbs, and provide mechanistic insight into the anatomical foundation of Gegenbaur's gill arch hypothesis.**

## Introduction

Chondrichthyans are unique among extant jawed vertebrates in possessing appendages, known as branchial rays, which project laterally from their gill arches (Gillis et al., 2009a). This anatomy mirrors the configuration of paired fins (including limbs) and their proximal girdle, and led the comparative anatomist Carl Gegenbaur to propose that paired fins evolved by transformation of a gill arch, with the epi- and ceratobranchial cartilages of the gill arch giving rise to the girdle, and branchial rays giving rise to the fin proper (Gegenabur, 1878). This hypothesis of serial homology (Fig. 1) would predict that the gill arches of chondrichthyans and the paired fins/limbs of jawed vertebrates share axial patterning mechanisms. However, while a great deal is known about the molecular basis of paired fin and limb patterning (Zeller et al., 2009), comparable data on axial patterning of chondrichthyan gill arches and branchial rays are lacking.

Limbs are patterned, in part, by a signalling centre known as the zone of polarizing activity (ZPA): a population of *sonic hedgehog* (*Shh*)-expressing cells in the posterior limb bud mesenchyme that signals to adjacent mesenchymal cells and to the overlying apical ectodermal ridge (Pearce et al., 2001), and that functions both in the establishment of the anteroposterior axis of the limb bud, and in the proliferative expansion of limb endoskeletal progenitors (Riddle et al., 1993; Towers et al., 2008;

Zhu et al., 2008). We previously demonstrated that the branchial rays of chondrichthyans also develop under the influence of a *Shh*-expressing signalling centre (Gillis et al., 2009b; Gillis et al., 2011), though the precise function of this signalling centre remains unclear. To address this, we have used gene expression analysis, fate mapping and loss-of-function experiments to investigate the function of the gill arch Shh signalling in the little skate (*Leucoraja erinacea*). We demonstrate that gill arch Shh signalling functions similarly to the limb bud ZPA, both in the establishment of the skate gill arch anteroposterior axis, and in the proliferative expansion of branchial ray endoskeletal progenitors.

## Results and discussion

### *Shh signalling in skate gill arch development*

In order to identify the source and targets of chondrichthyan gill arch Shh signaling, we characterized the expression of *Shh* and *Patched2* (*Ptc2*, a readout of Shh signalling – Pearce et al., 2001) by mRNA *in situ* hybridisation in skate embryos. In vertebrate embryos, pharyngeal arches are delineated by an iterative series of endodermal pouches that outpocket from the foregut and contact overlying pharyngeal ectoderm. In fishes, endodermal pouches fuse with overlying ectoderm, giving rise to gill slits, and leaving, between presumptive gill slits, pharyngeal arches filled with neural crest-derived mesenchyme and a central mesodermally-derived core (Graham, 2001). In skate embryos at stage 22 (Ballard et al., 1993) (Fig. 2A), *Shh* expression is observed in the region of the pharyngeal gill slits and pouches (Fig. 2B). Expression analysis on paraffin sections reveals that *Shh* transcripts localize to the posterior pharyngeal arch epithelium (Fig. 2C,D), consistent with previous reports of *Shh* expression in the posterior hyoid arches of chick (Wall and Hogan, 1995) and zebrafish (Richardson et al., 2012) embryos. Analysis of *Ptc2* expression at stage 22 indicates that pharyngeal arch Shh signal is transduced posteriorly within the developing gill arches, in pharyngeal arch epithelium, mesenchyme and in the mesodermally-derived core (Fig. 2E).

By stage 27, all pharyngeal arches have formed, and the hyoid and gill arches are expanding laterally (Fig. 2F). At this stage, *Shh* expression is restricted to the epithelium along the leading edge of the expanding hyoid and gill arches (Fig. 2G-I), with *Shh*-expressing cells having the appearance of a ridge (the gill arch epithelial ridge, GAER). The GAER is reminiscent of the apical ectodermal ridge (AER) of the

developing fin and limb buds, and we have previously shown that, like the fin/limb bud AER, the GAER also expresses the gene encoding the signaling molecule Fgf8 (Gillis et al., 2009b). *Ptc2* expression reveals that GAER Shh signal is asymmetrically transduced in posterior-distal arch mesenchyme, as well as in cells within the mesodermally-derived core and distal arch epithelium (Fig. 2J). By stage 29, the hyoid and gill arches continue to expand laterally, and have taken on a pronounced posterior curvature (Fig. 2K). *Shh* expression persists in the GAER of the hyoid arch and gill arches (Fig. 2L-N), and *Ptc2* expression indicates transduction of GAER Shh in posterior-distal arch mesenchyme, a few cells at the distal tip of the mesodermally-derived core, and in the GAER and adjacent epithelium (Fig. 2O). At stages 27 and 29, cells of the GAER are distinguishable as a pseudostratified epithelial ridge, approximately 5-6 cells in diameter (Fig. 2P). By stage 30, anlagen of pharyngeal endoskeletal elements appear (Gillis et al., 2009a).

In summary, the GAER is a *Shh*-expressing signaling centre that spans the leading edge of the expanding skate hyoid and gill arches. GAER *Shh* expression originates within posterior pharyngeal arch epithelium, and persists through lateral expansion of the hyoid and gill arches, resolving into a morphologically distinct pseudostratified epithelial ridge, while signaling to posterior arch mesenchyme and epithelium. Thus, while the GAER is distinct from the limb bud ZPA at the tissue level (the former is epithelial, while the latter is mesenchymal), both provide a posteriorly localized source of Shh signal that is transduced in adjacent mesenchymal and epithelial cell populations.

*Shh-responsive mesenchyme gives rise to branchial rays*

The gill arch endoskeleton of chondrichthyans consists of proximal epi- and ceratobranchial cartilages, and a series of branchial rays projecting laterally from these (Fig. 3A,B). In the tetrapod limb, it has been demonstrated that ZPA Shh-responsive mesenchyme contributes extensively to the distal limb skeleton (Ahn and Joyner, 2004), and these elements exhibit morphological defects following loss of Shh signaling (Riddle et al., 1993; Chiang et al., 2001; Ros et al., 2003; Stopper and Wagner, 2007; Towers et al., 2008; Zhu et al., 2008). To test the endoskeletal fate of GAER Shh-responsive mesenchyme, we labeled this cell population by microinjecting CM-DiI subjacent to the GAER of gill arches in skate embryos at stages 27 and 29 (Fig. 3C,D – compare injection with *Ptc2* expression in Fig. 2J). Injected embryos were reared until stages 31-32 (~8-10 weeks of development,

when gill arches and branchial rays have differentiated,), and analyzed for the presence and distribution of CM DiI-positive chondrocytes in histological sections of the gill arch endoskeleton.

Histological analysis of gill arches of skates with labeled GAER Shh-responsive mesenchyme revealed the presence of DiI-labeled chondrocytes in the branchial rays (100% of examined individuals; n=5 for CM-DiI labeling at stage 27, and n=5 for CM-DiI labeling at stage 29) (Fig. 3E). In individuals labeled at stage 27, DiI-positive chondrocytes were distributed broadly throughout the branchial rays, whereas individuals labeled at stage 29 possessed DiI-positive chondrocytes predominantly in the distal tips of the rays. These data indicate that GAER Shh-responsive mesenchymal cells contribute to branchial rays, which are the elements that Gegenbaur serially homologized with the paired fin/limb endoskeleton (Fig. 1).

*Shh polarizes and maintains proliferative expansion of gill arch endoskeletal progenitors*

In the tetrapod limb, Shh signaling from the ZPA functions both in the establishment of the limb bud anteroposterior axis, and in the maintenance of proliferative expansion of limb endoskeletal progenitors (Towers et al., 2008; Zhu et al., 2008). To test the patterning function of Shh signalling during skate gill arch development, we conducted a series of loss-of-function experiments by *in ovo* injection of the hedgehog signalling antagonist cyclopamine (Chen et al., 2002). Skate eggs were injected with cyclopamine to a final concentration of ~20μM, at either stage 22, 27 and 29, and were then reared until endoskeletal differentiation (~8-12 weeks). As with digit number in mice (Zhu et al., 2008) and salamanders (Wagner and Stopper, 2007), successively earlier loss of Shh signalling resulted in a progressively greater reduction in the number of branchial rays on each arch. Specifically, cyclopamine treatment at stages 22 and 27 resulted in significant reductions in branchial ray number, relative to controls, but there was no significant reduction in branchial ray number with cyclopamine treatment at stage 29 (Fig. 4A,B). We postulated that reductions in branchial ray number were due to reduced proliferation of gill arch mesenchyme in the absence of gill arch Shh signalling, and to test this, we conducted a series of EdU (Salic and Mitchison, 2008) incorporation experiments. Embryos at stage 27 were reared *ex ovo* in either 20μM cyclopamine or DMSO in seawater for 24 hours, prior to intraperitoneal microinjection with EdU. Injected embryos were left to develop for a further 24 hours, fixed and analyzed for EdU

retention in gill arch mesenchyme. Embryos treated with cyclopamine showed a significant reduction in the proportion of EdU-positive nuclei in gill arch mesenchyme, relative to controls, indicative of reduced DNA replication (and hence, cell proliferation) in the absence of Shh signalling (Fig. 4C). Together with our fate mapping data, these findings indicate that gill arch Shh signalling functions, in part, to maintain proliferative expansion of branchial ray progenitors during gill arch development.

Finally, we noted a striking anteroposterior patterning defect in the gill arches of the earliest cyclopamine-treated skate embryos. Chondrichthyan gill arches exhibit a clear anteroposterior polarity, with branchial rays invariably articulating with the epi- and ceratobranchial cartilages along their posterior margins (Gillis et al., 2009a). In skate embryos treated with cyclopamine at stage 22, the epi- and ceratobranchial cartilages were severely misshapen, consistently lacking evidence of an anteroposterior axis, with branchial rays articulating along their midlines (n=4/7) (Fig. 4D). Notably, this patterning defect was not observed in any embryos treated with cyclopamine at stages 27 (n=0/7) or 29 (n=0/9). These findings suggest that, in addition to its prolonged role in maintaining gill arch proliferative expansion, Shh signalling also functions early in gill arch development, to establish gill arch anteroposterior polarity.

*Conclusion*

Gegenbaur's gill arch hypothesis of paired fin origins is often regarded as the flawed alternative to the lateral fin fold hypothesis of Thacher (1877), Mivart (1879) and Balfour (1881), which purports that paired fins evolved from a bilateral median fin-like structure. While neither the gill arch nor lateral fin fold hypotheses are supported by paleontological data (Coates, 2003), consensus has largely shifted toward the latter, owing to the discovery of shared expression of developmental patterning genes between paired and dorsal median fins (Freitas et al., 2006; Dahn et al., 2007). Our demonstration of a dual role for Shh signaling in patterning the endoskeleton of chondrichthyan gill arches points to a common molecular mechanism underlying the axial patterning of branchial rays and paired fins/limbs, and highlights chondrichthyan branchial rays as an important feature in the evolutionary story of gnathostome paired appendages. Conserved developmental mechanisms are generally regarded as the basis of serial homology (Roth, 1984; Wagner, 1989, 2007), though it remains to be determined whether developmental mechanisms shared by branchial rays and

paired fins/limbs reflect conservation, parallel evolution (i.e. the independent co-option of deeply conserved developmental mechanisms, or “deep homology”) or convergent evolution (Hall, 2003; Shubin et al., 2009). In the absence of paleontological data illustrating the step-wise acquisition of the paired fin endoskeleton, comparative studies of axial patterning mechanisms in diverse vertebrate appendages – e.g. fins/limbs, branchial rays, median fins and external genitalia (Cohn, 2011) – will allow us to formulate testable hypotheses of nested relationships among body plan features, in order to explain morphological similarity by extent of shared developmental information.

## Materials and methods

### *Embryo collection and fate mapping*

Skate (*Leucoraja erinacea*) eggs were obtained at the Marine Biological Laboratory (Woods Hole, MA, USA) and maintained in a flow-through seawater system at ~17°C. CM-DiI fate mapping experiments were carried out as described (Gillis et al., 2012). All animal work complied with protocols approved by the Institutional Animal Care and Use Committee at the MBL. Embryos were fixed in 4% paraformaldehyde in phosphate-buffered saline (PBS) overnight at 4°C, rinsed three times in PBS, dehydrated into methanol and stored at -20°C.

### *Histology and mRNA in situ hybridization*

Embryos were embedded in paraffin wax and sectioned as described (O’Neill et al., 2007). Sections of CM-DiI-labelled embryos were counterstained with DAPI. *In situ* hybridization experiments for *L. erinacea Shh* (GenBank Accession Number EF100667) and *Ptc2* (GenBank Accession Number EF100663) were performed as described (Gillis et al., 2012).

### *In ovo cyclopamine treatment and skeletal preparations*

To achieve a final *in ovo* cyclopamine concentration of ~20μM, 25μL of a 9mM stock solution of cyclopamine in DMSO was injected into 25 skate egg cases each at stages 22, 27 and 29, using a syringe and 30 gauge needle. This volume was determined based on a mean egg volume of ~10mL. For controls, an equivalent volume of DMSO alone was injected. Embryos were reared for 8-12 weeks.

Surviving embryos (n=7, 7 and 9 for cyclopamine treatment at stage 22, 27 and 29, respectively) were analysed for skeletal defects by wholemount skeletal preparation (Gillis et al., 2009a).

*EdU incorporation assay*

For 5-ethynyl-2-deoxyuridine (EdU) incorporation experiments, stage 27 embryos were removed from their egg cases, and reared in 10cm diameter petri dishes in either 20μM cyclopamine in seawater (n=5), or in seawater with an equivalent volume of DMSO (n=5). After 24 hours, embryos received an intraperitoneal microinjection of ~0.5μL of 5mM EdU (ThermoFisher Scientific, Waltham, MA, USA) in 1X PBS, using a pulled glass capillary needle and a Picospritzer pressure injector. Embryos were then returned to their cyclopamine/DMSO baths for a further 24 hours. EdU-injected embryos were fixed and processed for histology as described above. EdU was detected in sections using the Click-iT EdU Alexa Fluor 488 Imaging Kit (ThermoFisher Scientific, Waltham, MA, USA), and sections were counterstained with DAPI. Counts of EdU-positive nuclei were carried out manually, using the Cell Counter plugin for ImageJ. Mean proportion of EdU-positive nuclei in gill arch mesenchyme was calculated for three individuals per treatment or control (with cell counts from three consecutive sections per individual), and statistical significance was determined by unpaired T test.

**Acknowledgements**

The authors acknowledge the support of Dr. Kate Rawlinson, Prof. Richard Behringer, Prof. Alejandro Sánchez Alvarado, Prof. Jonathan Henry, Dr. Deirdre Lyons, the MBL embryology community and the staff of the MBL Marine Resources Center.

**Competing interests**

No competing interests declared.

**Author contributions**

JAG conceived the study. JAG designed and conducted all experiments, analyzed all data and wrote the manuscript (with input from BKH).

**Funding**

This research was supported by a Royal Society University Research Fellowship [UF130182 to JAG], by Plum foundation John E. Dowling and Laura and Arthur Colwin Endowed Summer Research Fellowships at the Marine Biological Laboratory to JAG, by a grant from the University of Cambridge Isaac Newton Trust to [14.23z to JAG], and by a grant from the Natural Sciences and Engineering Research Council of Canada [A5056 to BKH].

## References

**Ahn, S. and Joyner, A.L.** (2004) Dynamic changes in the response of cells to positive hedgehog signaling during mouse limb patterning. *Cell* **188**, 505-516.

**Balfour, F.M.** (1881) On the development of the skeleton of the paired fins of Elasmobranchii, considered in relation to its bearing on the nature of the limbs of the Vertebrata. *Proc. Zool. Soc. Lond.* **1881**, 656-671.

**Ballard, W.W., Mellinger, J. and Lechenault, H.** (1993) A series of normal stages for development of *Scyliorhinus canicula*, the lesser spotted dogfish (Chondrichthyes: Scyliorhinidae) *J. Exp. Zool.* **267**, 318-336.

**Chiang, C., Litingtung, Y., Harris, M.P., Simandl, B.K., Li, Y., Beachy, P.A. and Fallon, J.F.** (2001) Manifestation of the limb prepattern: limb development in the absence of sonic hedgehog function. *Dev. Biol.* **236**, 421-435.

**Chen, J.K., Taipale, J., Young, K.E., Maiti, T. & Beachy, P.A.** (2002) Small molecule modulation of Smoothened activity. *Proc Nat'l Acad Sci U.S.A.* **99**, 14071-14076.

**Coates, M.I.** (2003) The evolution of paired fins. *Theor. Biosci.* **122**, 266-287.

**Cohn, M.J.** (2011) Development of external genetalia: conserved and divergent mechanisms of appendage patterning. *Dev. Dyn.* **240**, 1108-1115.

**Dahn, R.D., Davis, M.C., Pappano, W.N. and Shubin, N.H.** (2007) Sonic hedgehog function in chondrichthyan fins and the evolution of appendage patterning. *Nature* **445**, 311-314.

**Freitas, R., Zhang, G. and Cohn, M.J.** (2006) Evidence that mechanisms of fin development evolved in the midline of early vertebrates. *Nature* **441**, 1033-1037.

**Gegenbaur, C** (1878) *Elements of Comparative Anatomy.* London, UK: Macmillan.

**Gillis, J.A., Dahn, R.D. and Shubin, N.H.** (2009a) Chondrogenesis and homology of the visceral skeleton in the little skate, *Leucoraja erinacea* (Chondrichthyes: Batoidea). *J. Morphol.* **270**, 628-643.

**Gillis, J.A., Dahn, R.D. and Shubin, N.H.** (2009b) Shared developmental mechanisms pattern the vertebrate gill arch and paired fin skeletons. *Proc. Nat'l Acad. Sci. U.S.A.* **106**, 5720-5724.

**Gillis, J.A., Rawlinson, K.A., Bell, J., Lyon, W.S., Baker, C.V. and Shubin, N.H.** (2011) Holocephalan embryos provide evidence for gill arch appendage reduction and opercular evolution in cartilaginous fishes. *Proc. Nat'l Acad. Sci. U.S.A.* **108**, 1507-1512.

**Gillis, J.A., Modrell, M.S., Northcutt, R.G., Catania, K.C., Luer, C.A. and Baker, C.V.H.** (2012) Electrosensory ampullary organs are derived from lateral line placodes in cartilaginous fishes. *Development* **139**, 3142-3146.

**Graham, A.** (2001) The development and evolution of the pharyngeal arches. *J. Anat.* **199**, 133-141.

**Hall, B.K.** (2003) Descent with modification: the unity underlying homology and homoplasy as seen through an analysis of development and evolution. *Biol. Rev.* **78**, 409-433.

**Mivart, S.G.** (1879) Notes on the fins of Elasmobranchs, with considerations on the nature and homologies of vertebrate limbs. *Trans. Zool. Soc. Lond.* **10**, 439-484.

**O'Neill, P, McCole, R.B. and Baker, C.V.H.** (2007) A molecular analysis of neurogenic placode and cranial sensory ganglion development in the shark, *Scyliorhinus canicula*. *Dev. Biol.* **304**, 156-181.

**Owen, R.** (1866) *Anatomy of Vertebrates I. Fishes and Reptiles*. London, U.K.: Longmans, Green, and Co.

**Pearce, R.V. Vogan, K.J. and Tabin, C.J.** (2001) *Ptc1* and *Ptc2* transcripts provide distinct readouts of Hedgehog signaling activity during chick embryogenesis. *Dev. Biol.* **239**, 15-29.

**Richardson, J., Shono, T., Okabe, M. and Graham, A.** (2012) The presence of an embryonic opercular flap in amniotes. *Proc. Biol. Sci.* **279**, 224-229.

**Riddle, R.D., Johnson, R.L., Laufer, E. and Tabin, C.J.** (1993) Sonic hedgehog mediates the polarizing activity of the ZPA. *Cell* **75**, 1401-1416.

**Ros, M.A., Dahn, R.D., Fernandez-Teran, M., Rashka, K., Caruccio, N.C., Hasso, S.M., Bitgood, J.J., Lancman, J.J. and Fallon, J.F.** (2003) The chick *oligozeugodactyly* (*ozd*) mutant lacks sonic hedgehog function in the limb. *Development* **130**, 527-537.

**Roth, V.L.** (1984) On homology. *Biol. J. Linn. Soc.* **22**, 13-29.

**Salic, A. and Mitchison, T.J.** (2008) A chemical method for fast and sensitive detection of DNA synthesis *in vivo*. *Proc Nat'l Acad Sci U.S.A.* **105**, 2415-2420.

**Shubin, N.H., Tabin, C.J. and Carrol, S.** (2009) Deep homology and the origins of evolutionary novelty. *Nature* **457**, 818-823.

**Stopper, G.F. and Wagner, G.P.** (2007) Inhibition of Sonic hedgehog signaling leads to posterior digit loss in *Ambystoma mexicanum*: parallels to natural digit reduction in urodeles. *Dev. Dyn.* **236**, 321-331.

**Thacher, J.K.** (1877) Median and paired fins, a contribution to the history of vertebrate limbs. *Trans. Connecticut Acad. Sci.* **3**, 281-308.

**Towers, M., Mahood, R. Yin, Y. and Tickle, C.** (2008) Integration of growth and specification in chick wing digit patterning. *Nature* **452**, 882-886.

**Wagner, G.P.** (1989) The biological homology concept. *Annu. Rev. Ecol. Syst.* **20**, 51-69.

**Wagner, G.P.** (2007) The developmental genetics of homology. *Nat. Rev. Genet.* **8**, 473-479.

**Wall, N. and Hogan, B.** (1995) Expression of bone morphogenetic protein-4 (BMP-4), bone morphogenetic protein-7 (BMP-7), fibroblast growth factor-8 (FGF-8) and sonic hedgehog (SHH) during branchial arch development in chick. *Mech. Dev.* **53**, 383-392.

**Zeller, R., Lopez-Rioz, J. and Zuniga, A.** (2009) Vertebrate limb development: moving towards integrative analysis of organogenesis. *Nat. Rev. Genet.* **10**, 845-858.

**Zhu, J., Nakamura, E., Nguyen, M.T., Bao, X., Akiyama, H. and Mackem, S.** (2008) Uncoupling sonic hedgehog control of pattern and expansion of the developing limb bud. *Dev. Cell.* **14**, 624-632.

**Figure legends**

**Figure 1: Hypothesis of gill arch-paired fin serial homology.** A shark head skeleton illustrating putative serial homology of the gill arch and pectoral fin skeleton. Gill arches (ga) and the pectoral girdle (pg) are coloured yellow; branchial rays (br) and the pectoral fin (pf) are coloured red (modified from Owen, 1866).

**Figure 2: Shh signaling during skate gill arch development. A.** At stage 22, **B.-D.** *Shh* is expressed in the developing gill arches, with transcripts localizing to posterior arch epithelium. **E.** *Ptc2* expression indicates that this signal is transduced in posterior gill arch mesenchyme, epithelium, and core mesoderm. **F.** By stage 27, **G.-I.** *Shh* expression has resolved into a ridge of epithelial cells (the gill arch epithelial ridge, GAER; black arrow) along the leading edge of the expanding hyoid and gill arches, and **J.** *Ptc2* expression indicates that this signal is transduced in posterior-distal mesenchyme, epithelium and core mesoderm. **K.** By stage 29, **L.-N.**

expression of *Shh* is maintained in the GAER, and **O.** *Ptc2* expression indicates sustained posterior-distal transduction of this signal in posterior-distal arch mesenchyme, epithelium and core mesoderm. **P.** The GAER is recognizable as a pseudostratified ridge of *Shh*-expressing epithelial cells. *m*, mandibular arch; *h*, hyoid arch; *1-5*, gill arch 1-5. Dashed lines in **B.**, **G.**, and **L.** indicate plane of section in **C.**-**E.**, **H.**-**J.** and **M.**-**O.**, respectively. Scale bars: A, F, K = 500µm; C, H, M = 30µm; P = 5µm.

**Figure 3: Shh-responsive gill arch mesenchyme gives rise to branchial rays. A.** Lateral view of the skate pharyngeal endoskeleton, showing branchial rays (*) projecting laterally from the hyoid and gill arches. **B.** Frontal view of a gill arch, showing branchial rays (br) articulating with the epibranchial (eb) and ceratobranchial (cb) cartilages. **C.-D.** CM-DiI was microinjected subjacent to the GAER, from stages 27-29. **E.** After 8-10 weeks of development, CM-DiI-positive chondrocytes were recovered in branchial rays. In **E.**, the epibranchial cartilage is false coloured red, and the branchial ray is false coloured yellow. *ey*, eye; *ot*, otic vesicle. Scale bars: A = 1.5mm; B = 1.25mm; C = 500µm; D–F = 30µm.

**Figure 4: A dual role for Shh signaling in gill arch anteroposterior patterning and proliferative expansion. A.** Successively earlier treatment with cyclopamine results in a progressively greater reduction in branchial ray number, with significantly fewer branchial rays following cylopamine treatment at stages 22 and 27 (mean number of branchial rays per arch +/- SEM; n=3 embryos per control or treatment; * indicates statistical significance at $p<0.05$). **B.** Example of a control (DMSO) arch, and arches from embryos treated with cyclopamine at stages 22, 27 and 29. **C.** EdU retention assays at stage 27 reveal reduced mesenchymal cell proliferation upon treatment with cyclopamine (mean proportion of EdU+ cells +/- SEM; n=3 embryos per control or treatment; * indicates statistical significance at $p<0.0001$). **D.** Embryos treated with cyclopamine at stage 22 also exhibit anteroposterior patterning defects. In dorsal view, branchial rays can be seen to articulate with the posterior margin of the epibranchial cartilage. Cyclopamine treatment at stage 22 results in a loss of anteroposterior polarity within the gill arches, with branchial rays articulating down the midline of the epibranchial (*). This defect is not observed following cyclopamine treatment at stage 27 or 29. In schematics in **D.**, the epibranchial is yellow, and branchial rays are red. Scale bars: B = 1.25mm; C = 30µm.

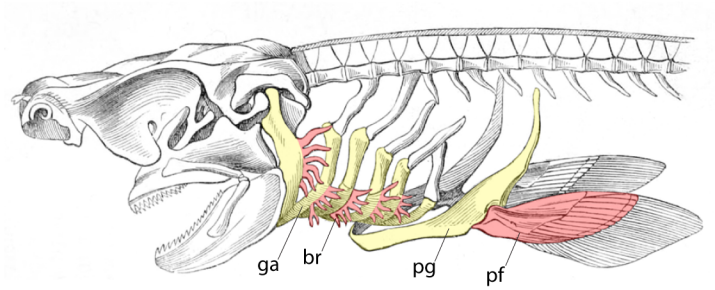


**Figure 1**

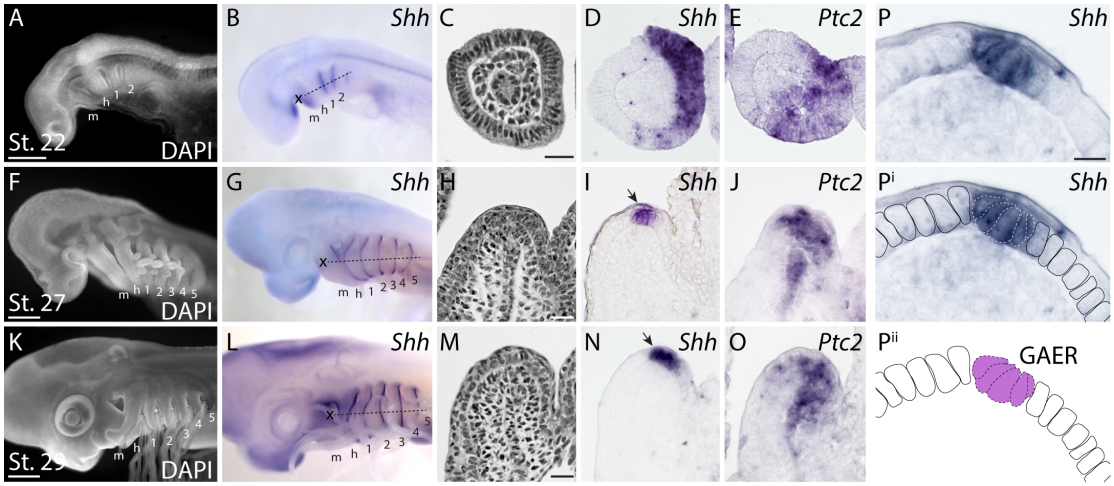
A
St. 22
DAPI
B
Shh
C
D
Shh
E
Ptc2
P
Shh
F
St. 27
DAPI
G
Shh
H
I
Shh
J
Ptc2
Pi
Shh
K
DAPI
L
Shh
M
N
Shh
O
Ptc2
Pii
GAER

**Figure 2**

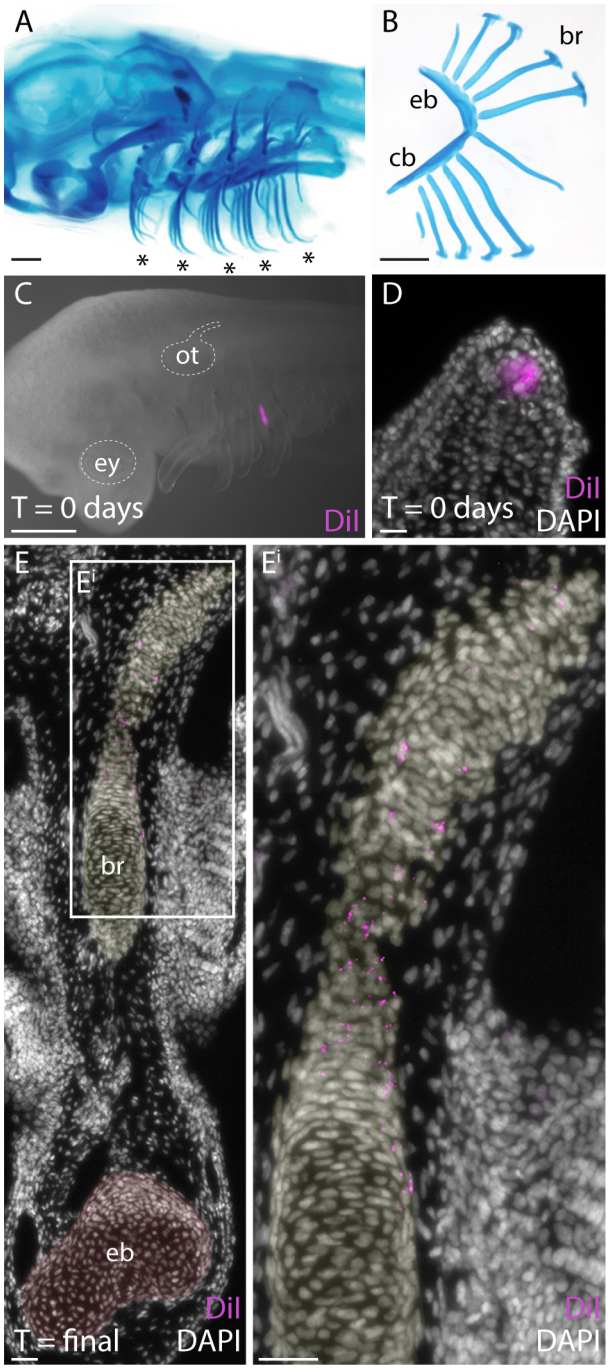
A
B
br
eb
cb
C
ot
ey
T = 0 days
DiI
D
T = 0 days
DiI
DAPI
E
Ei
br
eb
DiI
T = final
DAPI
Ei
DiI
DAPI

**Figure 3**

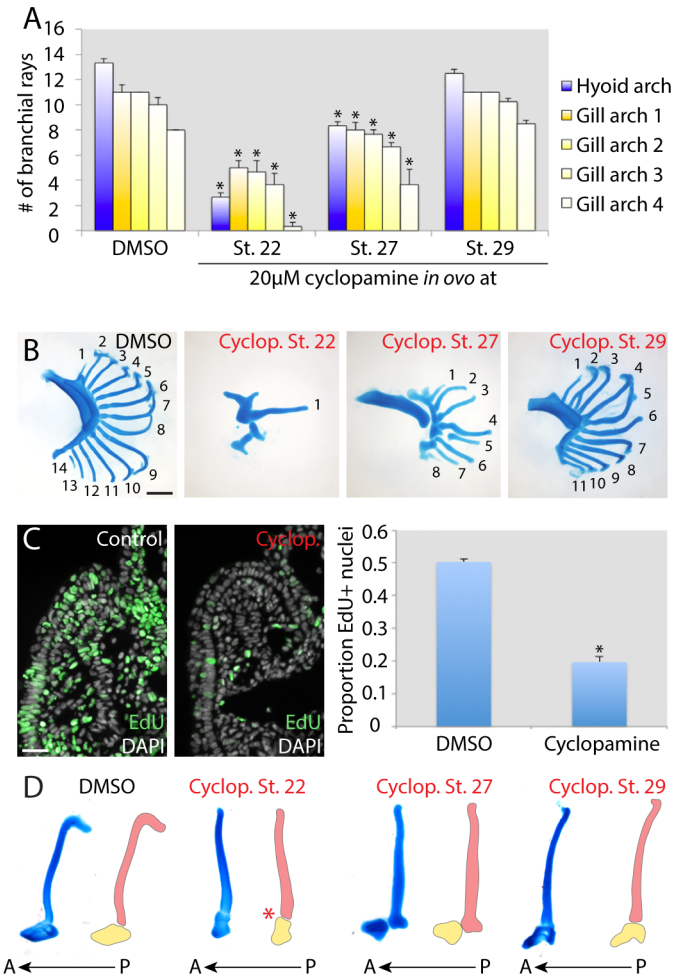
A
# of branchial rays
Hyoid arch
Gill arch 1
Gill arch 2
Gill arch 3
Gill arch 4
DMSO
St. 22
St. 27
St. 29
20µM cyclopamine in ovo at
B
DMSO
Cyclop. St. 22
Cyclop. St. 27
Cyclop. St. 29
C
Control
Cyclop.
EdU
DAPI
Proportion EdU+ nuclei
DMSO
Cyclopamine
D
DMSO
Cyclop. St. 22
Cyclop. St. 27
Cyclop. St. 29
A
P

**Figure 4**